A Novel Sublimable Mask Lift-Off Method for Patterning Thin Films

by

Matthias Erhard Bahlke

B.A. Physics (2009)
Bard College
B.S. Electrical Engineering (2009)
Columbia University

Submitted to the Department of Electrical Engineering and Computer Science
in partial fulfillment of the requirements for the degree of

Master of Science in Electrical Engineering and Computer Science

at the

MASSACHUSETTS INSTITUTE OF TECHNOLOGY

February 2011

Author .....
Department of Electrical Engineering and Computer Science
January 28, 2011

Certified by .....
Marc A. Baldo
Associate Professor of Electrical Engineering
Thesis Supervisor

Accepted by .....
Terry P. Orlando
Chair, Department Committee on Graduate Students

A Novel Sublimable Mask Lift-Off Method for Patterning Thin Films

by

Matthias Erhard Bahlke

Submitted to the Department of Electrical Engineering and Computer Science
on January 28, 2011, in partial fulfillment of the
requirements for the degree of
Master of Science in Electrical Engineering and Computer Science

Abstract

Photolithography's accuracy and scalability has made it the method for sub-micron-scale definition of single-crystal semiconductor devices for over half a century. Unfortunately, organic semiconductor devices are chemically incompatible with the types of resists, solvents, and etchants traditionally used. This work investigates the use of a chemically inert resist that relies on phase changes for lift-off patterning thin films of organic semiconductors and metals.

Thesis Supervisor: Marc A. Baldo
Title: Associate Professor of Electrical Engineering

Acknowledgments

First and foremost I'd like to thank my research advisor, Marc, for his ideas, interest and encouragement—I'd have been unable to complete this work without his help. I'd also like to thank Hiroshi Mendoza for his sustained optimism and undying motivation and Jon Mapel for his assistance with scaling and market evaluation. Nicholas Thompson has been very helpful with his continued interest, feedback and suggestions. Apoorva Murarka saved us a lot of time donating one of his old MEMS stamps and assisting with making the first of my own. Phil Reusswig and Priya Jadhav provided necessary and much-appreciated assistance with experimental design. I can't thank Jason Sussman enough for his comprehensive attention to detail in reviewing the manuscript. I'd like to acknowledge The rest of The Soft Semiconductor Group that I've worked along side of: Jiye Lee, Carlijn Mulder, Amador Velázquez, Carmel Rotschild, Tim Heidel, Paul Azunre, Jean Anne Currivan and Allen Yin for assistance and helpful discussions along the way.

I'm indebted to John Kymissis and the Columbia Laboratory for Unconventional Electronics for helping me realize that graduate school in engineering was right for me. Outside of those that assisted with theory and experimental work, I'd like to thank my mother and father for their support as well as my brother and sister, George and Marlene.

Contents

1 Introduction **13**

1.1 Organic Light-Emitting Diode Displays 14

1.1.1 Current Commercial Status 14

1.1.2 Structure of an OLED 15

1.2 Motivations for an Alternative Patterning Process 16

1.2.1 Fine-Metal Masks 16

1.2.2 Inkjet Printing 17

1.2.3 Photolithographic Processes Involving Solvents 18

2 The Sublimable Mask Lithographic Process **19**

2.1 Theory of Practice 19

2.2 Process Flow 21

3 Proof of Concept **23**

3.1 Required Demonstration 23

3.2 Experimental Setup 24

3.2.1 Patterning the Resist with Resistive Heating 26

3.2.2 Patterning the Resist with a Stamp 29

3.3 Patterning the Resist Photolithographically 34

4 Conclusion **35**

A Molecules Used in this Work **37**

List of Figures

1-1 Dimensions of subpixels making up each of the 2 million pixels in a 32-inch HDTV. The area obstructing the top of the pixel is from the driving transistors. 15

1-2 A fine-metal mask used for arrays of OLED subpixels[40]. 17

2-1 General phase diagram. The arrow shows the ideal region of operation with respect to sublimation lithography. Deposition of the mask takes place along the low temperature region of the arrow and sublimation and lift-off take place along the higher temperature region of the arrow. 20

2-2 Phase diagram reflecting full process flow parameters. The defining of the mask pattern is performed immediately prior to the deposition of the thin film. 21

2-3 Simplified process flow for sublimation lithography. (not to scale) (a) Begin with a cooled substrate to facilitate resist deposition. (b) Deposit resist. (c) Selectively pattern resist. (d) Deposit desired thin film. (e) Lift-off resist leaving patterned thin film. (f) Repeat as necessary to complete device. 22

3-1 The side of the evaporation chamber showing the feedthroughs and liquid nitrogen reservoir. 25

3-2 Flange making up the bottom of the liquid nitrogen reservoir. The substrate holding plate is bolted in with a glass sample tighyly secured. The thermocouple can be seen towards the top of the image mounted with a bolt. 26

3-3 CO_2 phase diagram data[4], extrapolated by Nicholas Thompson for the low pressures and temperatures required for this process. Key points are noted. 27
3-4 The pattern of the ITO used in resistive heating experiments. The black regions are ITO; the white regions are bare glass. 29
3-5 A mask of CO_2 patterned for a 100μm-wide line. The substrate holder is rigged with probe-tipped clips for electrical contact. 30
3-6 An exmaple of photoluminescence from a 100μm-wide line of DCJTB-doped Alq_3(*top*), and photoluminescence(*bottom-left*) and a micrograph(*bottom-right*) from a 100μm-wide line of Alq_3 patterned by resistive heating of ITO. 31
3-7 A micrograph from a 100μm-wide line of silver patterned by resistive heating of ITO 32
3-8 A micrograph of the 115μm-tall pillar SU-8 stamp(*top*) used to pattern circles of Alq_3(*bottom*) 33

A-1 Aluminium tris(quinolin-8-olate) (Alq_3)[6] 37
A-2 Carbon dioxide (CO_2) 37
A-3 4-(Dicyanomethylene)-2-tert-butyl-6-(1,1,7,7-tetramethyljulolidin-4-yl-vinyl)-4H-pyran (DCJTB)[6] 38
A-4 SU-8 Photoresist[6] 38

List of Tables

1.1 Typical display specifications of current competing mobile displays.[3][5][1] 14

Chapter 1

Introduction

ORGANIC semiconductors devices are thin and efficient, but have yet to live up to their full potential as the basis of cheap optoelectronic devices. The problem is not one of material costs, but of obstacles to patterning for large-scale fabrication. This work provides an alternative manufacturing technique employing phase-change resists that may allow for the retirement of the fine-metal-masking methods currently used.

This chapter introduces the working principles, commercial status and potential of organic light-emitting diodes. It also explains how a dry lithographic process could overcome present challenges in scaling up production of OLEDs on larger sizes of mother glass.

Chapter two introduces the sublimable mask patterning idea and provides a step-by-step overview of the process.

Chapter three describes the approach and design of a proof-of-concept implementation using carbon dioxide ice as the resist.

Chapter four summarizes the results and describes options for large-scale patterning of the resist and the under- and overlying thin films. We briefly discusses limitations of techniques and the feasibility of such a process.

Table 1.1: Typical display specifications of current competing mobile displays.[3][5][1]

Display	Size (in)	Resolution	Technology	Maximum ppi
Apple iPhone Retina	3.5	960x640	LCD	326
Samsung AMOLED	3.5-4.3	800x480	AMOLED	260
Super LCD	3.5-4	800x480	LCD	260

1.1 Organic Light-Emitting Diode Displays

A 32-inch full high-definition television (HDTV) requires a pixel size of a 370μm-per side square further broken up into 3 subpixels: one for red, one for green and one for blue to reproduce the necessary colors required for full-color. Having features with dimensions of about 120μm necessitates patterning accuracies on the order of 10μm or less. For larger displays of the same resolution the pixel dimensions are larger and for smaller displays the definition is even tighter.

The highest resolution displays are found in mobile electronics like smartphones. They must reproduce great amounts information clearly on a screen of about 4 inches or less. The size, resolutions and pixel-per-inch (ppi) specifications of some of today's best displays are shown in table 1.1. 326ppi corresponds to a pixel pitch of about 80μm; 250ppi is more like 100μm. OLED manufacturers are at present unable to realize pixel pitches less than 100μm due to the problems laid out in section 1.2.

1.1.1 Current Commercial Status

OLED TVs are currently available, but only in 11-inch and 15-inch and not in full high-definition. Samsung is the OLED industry leader and will open a new $2.1 billion 5.5th-generation 5.5 OLED factory in the summer of 2011 to produce larger active-matrix OLED HDTVs[13][31]. Samsung will also increase its yearly investment in OLED technology by a factor of four from 2010 to 2011, about $4.8 billion, matching its investment in liquid crystal display technology [32].

The current organic electronics market stands at almost $2 billion and is expected to increase to $5.5 billion by 2015[14][15]. In 2010 Samsung Mobile Display announced

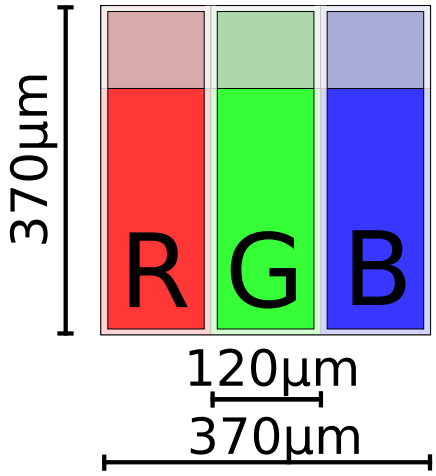

Figure 1-1: Dimensions of subpixels making up each of the 2 million pixels in a 32-inch HDTV. The area obstructing the top of the pixel is from the driving transistors.

that after years of investment, the OLED division is now profitable[27]. It is of interest here to note that the market contribution from televisions is negligible at this time, so there is much room for growth. Reducing the cost of OLED displays by solving yield and scaling complications is key. It is expected that by 2015, OLED HDTVs alone will be a $2 billion industry[14][24].

1.1.2 Structure of an OLED

OLEDs have a simple general structure and principle of operation. The first OLED demonstrated by C.W. Tang and S.A. VanSlyke in 1987[39] consisted of a monopolar transport layer and an emissive layer sandwiched between a transparent anode and an alloyed metal cathode. Today's OLEDs are a little more complicated: they make use of both singlet and triplet excitons for light generation[8], quadrupling efficiencies efficiencies relative to those devices relying on fluorescence alone[9]. Modern devices consist of an anode, hole-injection and hole-transport layers (HIL and HTL, respectively), host and dopant materials, electron-transport and electron-injection layers (ETL and EIL, respectively), blocking layers and a cathode. The anode or cathode must be transparent to allow light emission.

The reason for so many layers is to boost efficiency by increasing the probability of

charges recombining and, in turn, generating light. Electrical current is run through the device resulting in holes from the anode and electrons from the cathode meeting at a charge recombination interface.

1.2 Motivations for an Alternative Patterning Process

The only OLED displays that have reached profitability are in the small and mobile display markets. While larger displays are available, quantities and choice of products are limited and prohibitively expensive. The prices of larger displays would come down if the generation of display production (which corresponds directly to the size of the mother glass that the displays are grown on) were able to increase. This is currently limited by manufacturing processes.

The main competitor to OLEDs is liquid crystal displays (LCDs)(which are made in production plants rated about five generations higher than those of OLEDs). While an inherently more complicated design (involving polarizers, color filters, spacers, and liquid reservoirs[35]), their photolithography-compatible materials allow for simple scaling up of pixel electrode, transistor and color filter definition, thereby allowing larger mother glass production and consequently greater throughput.

1.2.1 Fine-Metal Masks

Current OLED patterning technology uses thin sheets of steel (see figure 1-2) that are used to define pixels during the thermal evaporation of organic semiconductors and metals. Placing these fine-metal masks (FMM) across sheets of glass to produce features on the order of 10μm introduces complications.

FMMs are fragile and, due to the nature of the masking process, must be cleaned after a number of growths to prevent defects caused by debris. This puts stress on the features of the mask and can result in tears and bending. They cost on the order of $200,000 and need to be replaced every one to two months. Moreover, tempera-

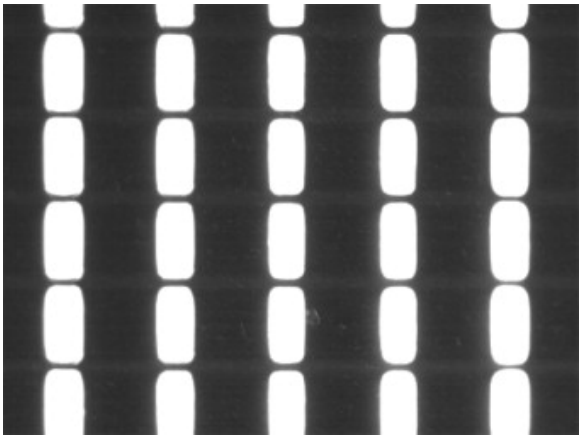

Figure 1-2: A fine-metal mask used for arrays of OLED subpixels[40].

ture deviations during the deposition can cause thermal expansion and contraction limiting the feature size.[38] Because the mask is not projected, but instead renders a 1:1 reproduction, incorporating multiple masks in a fabrication line requires tedious alignment.[21] This puts a bottleneck on throughput that, if eliminated or improved upon, would greatly reduce costs.

1.2.2 Inkjet Printing

Inkjet printing is another potential method for full-scale fabrication of organic electronics. is printing via inkjet. The oft-touted benefits include production without vacuum equipment, low operating costs and high material-use efficiency. An inket head operating on an XY-stage may also allow for simple pattern programming.

Unfortunately, inkjet printing has its own limitations. Such an inherently serial process requires and enormous number of printing heads to allow for reasonable throughput[37]. Even then, the organics in such a system must usually be put in solution before being printed requiring the replacement of many industry-leading small molecule organics with molecules with poorer performance. (It should be noted that this material limitation is not the case for molecular jet printing technologies[12].) Printing solutions also have issues with drop uniformity due to surface tension during the evaporation of the solvent[36][18][21], but this is actively being researched.

1.2.3 Photolithographic Processes Involving Solvents

Photolithography is widely used for patterning in the semiconductor industry, but is difficult to apply to the production of organic semiconductor devices. While solution-processable polymer devices have been photolithographically patterned[41], the resists, solvents and etchants are chemically incompatible with small-molecule organic semiconductors. More general photolithographic processes have required an intermediary polymer barrier [19] or the use of super-critical CO_2 [25]. The work proposed here investigates the use of a dry chemically inert phase-change resist that can be deposited and patterned in situ.

Chapter 2

The Sublimable Mask Lithographic Process

The concept and process of sublimation mask lithography are described in detail. While the idea and work here were developed independently, it is important to mention that similar methods were investigated by IBM in the late seventies[26] and early nineties[16] and by the Harvard Nanopore Group at Harvard University more recently[28][10][22]. But this is the first time that the dry nature of the method has been explored for use in patterning organic semiconductor devices.

2.1 Theory of Practice

Below a certain pressure and above a certain temperature, materials sublimae: they directly transition from solid to vapor without passing through a liquid phase. Deposition is the reverse transition. A phase diagram showing this region is seen in figure 2-1. As previously mentioned, a dry process is necessary for the production of organic semiconductors due to their sensitivity to traditional solvents. Depositing a material on a substrate whose phase can be easily changed between solid and vapor would make a versatile, clean and dry mask suitable for patterning.

The heat delivery requirements Q to sublime a solid of mass m, with specity heat

capacity c_V, and heat of sublimation h_s are

$$Q = m \int_{T_i}^{T_{sub}} c_V \mathrm{d}T + m h_S [20] \tag{2.1}$$

$$= m(c_V \Delta T + h_S) \tag{2.2}$$

Because the change in temperature ΔT (the change from the initial temperature T_i to the sublimation point T_{sub} required to bring the mask to the sublimation point is no more than 30°C, c_V is much less than its room temperature value of 37.1 J/molK[33] for the temperature regions of interest here and h_S is 26.1kJ/mol[7] for carbon dioxide, most of the heat going into the mask is required of sublimation rather than temperature increase, so

$$Q = m(c_v \Delta T + h_S) \approx m h_S \tag{2.3}$$

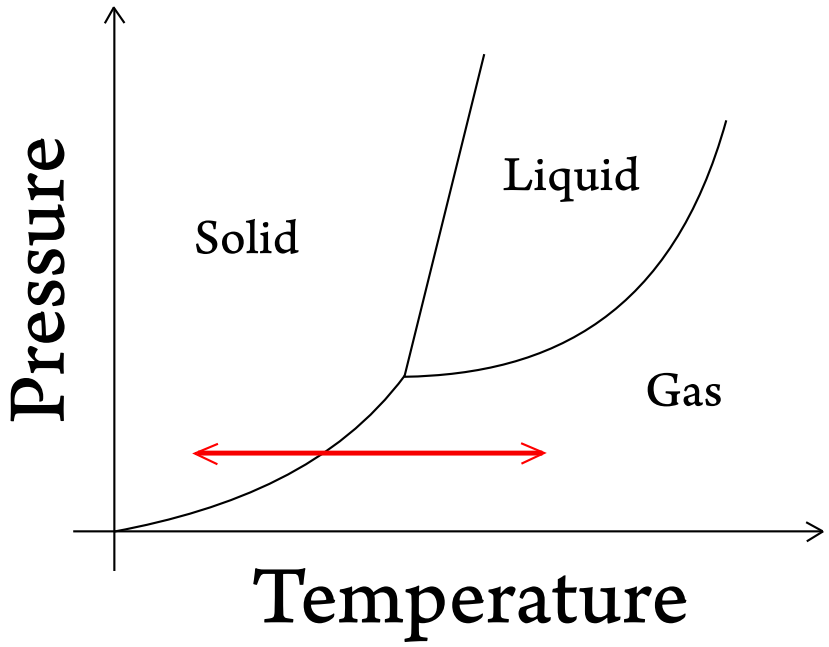

Figure 2-1: General phase diagram. The arrow shows the ideal region of operation with respect to sublimation lithography. Deposition of the mask takes place along the low temperature region of the arrow and sublimation and lift-off take place along the higher temperature region of the arrow.

2.2 Process Flow

In practice, there are other necessary considerations. Heat exchange with gas molecules at higher pressures causes the temperature to significantly fluctuate. The mask material would be very ineffective at the sublimation point due to the heat capacity and heat of deposition. The system temperature must therefore be kept significantly below this critical point for the resist material to be perform as intended. To raise the temperature of the sublimation point, the mask is deposited at a higher pressure to ensure that a higher portion of the gas is solidified. The pressure is later reduced for the deposition of the thin film. Figure 2-2 shows an updated phase diagram to reflect these details.

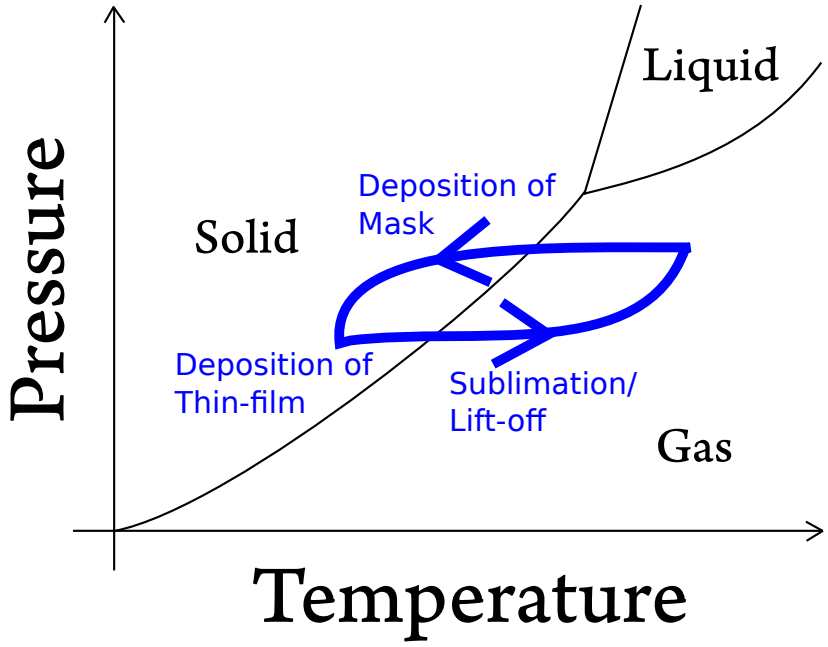

Figure 2-2: Phase diagram reflecting full process flow parameters. The defining of the mask pattern is performed immediately prior to the deposition of the thin film.

With the substrate at higher pressures and low temperature (so as to be well inside the solid portion of the phase diagram), the resist gas flows at and across the substrate where much of it deposits on the surface (part (a) and (b) of figure 2-3. Next, the mask is selectively patterned exposing the substrate to allow for the imminent neat films of the desired material to remain as intended post lift-off (part (c)). The thin film

is then grown over the mask at high-vacuum (part(d)). Following this, the substrate temperature is brought up to sublime away the mask which carries the undesired regions of thin film along with it (part(e)). These steps can be performed again and again as needed to build multi-layer devices.

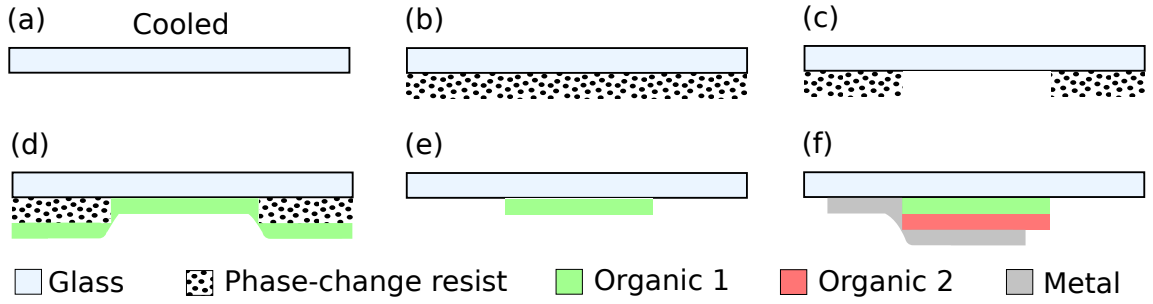

Figure 2-3: Simplified process flow for sublimation lithography. (not to scale) (a) Begin with a cooled substrate to facilitate resist deposition. (b) Deposit resist. (c) Selectively pattern resist. (d) Deposit desired thin film. (e) Lift-off resist leaving patterned thin film. (f) Repeat as necessary to complete device.

Chapter 3

Proof of Concept

THE resist is patterned two ways in the sections that follow. Photolithography is the third seemingly more elegant method and is considered, but found to be impractical for the proof-of-concept material used.

3.1 Required Demonstration

A small research-scale investigation is necessary to gauge the practicality of a full-scale sublimation patterning implementation. The basic principals of operation must be demonstrated and fundamental limitations must be observed. If realizable, the accuracy, repeatability, and resolution must be evaluated. Commercialization would require evidence of 10μm or smaller accuracy, as mentioned previously, as well as some proof of yield and high throughput.

This work is proof of principle for the fabrication of small-molecule organic semiconductor devices. An existing thermal evaporator served as a testbed for the original concept and all deviations therefrom. It was modified and refashioned as necessary to accommodate improvements upon steps of the process or to approach parts of the process from different angles. Full proof of commercializability would require a full-scale evaporator built from the ground up with sublimable mask lift-off patterning in mind, rather than a small research-scale system.

3.2 Experimental Setup

The experimental setup had to allow sufficient control of the process parameters outlined in section 2.2. We have a thermal evaporator attached to a glovebox, designed and built by Angstrom Engineering, that was easily modified to meet the processes needs. The dry and inert nitrogen environment of the glovebox is crucial to avoid water condensation on the substrate.

No substrate cooling was in place, so the rotating substrate holder was replaced with a liquid nitrogen reservoir. A flange with tapped holes allowing for a mounted substrate holder made up the bottom of the reservoir so the holder could be in nearly direct contact with the liquid nitrogen. Temperatures as low as -165°C were measured at pressures of 10^{-6} Torr with a type K thermocouple cemented to the surface of a like substrate. The difference between the surface temperature and that of boiling liquid nitrogen (-196°C) is attributed to the thermal conductivity of glass and steel. Indium foil inserted between each mating surface improves thermal conductivity. More traditional cryogenic thermal greases were abandoned because of their high photoluminescence and difficulty to cleanly work with in the glovebox.

Four feedthroughs (figure 3-1)allowed for observation and finer control of the frozen mask: a feedthrough for the aforementioned thermocouple, a four-pin electrical feedthrough, a 1/4" steel tube feedthrough, and a universal serial bus (USB) feedthrough. These allowed for temperature measurement, current sourcing (which will be elaborated on in 3.2.1), gas flow for resist deposition, and use of USB peripherals respectively. A USB hub with an attached light and webcam allowed for in situ optical observation.

A substrate holder was machined out of aluminum. Holes in the corners allowed for direct mounting to the bottom flange of the reservoir, while clips for securing the substrate and any electrical probes were located along the perimeter, as seen in figures 3-2 and 3-5. The center, though, was left in tact and smooth to minimize thermal resistance.

Just below the holder, a copper tube is connected to the 1/4" steel tube feedthrough

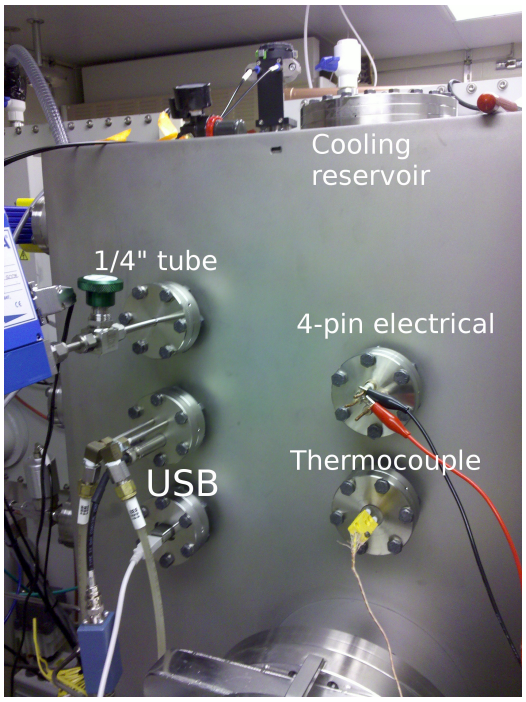

Figure 3-1: The side of the evaporation chamber showing the feedthroughs and liquid nitrogen reservoir.

and aimed at the substrate for CO_2 gas flow. The camera is clipped to this tube out of the way of organic material sources and thin film thickness sensors. A mass flow controller is connected on the outside end of this tube for gas flow rate control.

Carbon Dioxide as a Resist

Carbon dioxide is a natural choice for a sublimation resist. It is chemically inert, and its sublimation point is easily accessible with to a thermal evaporator equipped with liquid nitrogen cooling and simple heaters. As phase data was not readily available for the low pressure and temperature regime of this study, we extrapolated existing data with a thermodynamically fit trend to better understand how CO_2 would behave in our setup. CO_2's phase diagram and our extrapolation with pressure and temperature extremes of the experimental setup is shown in figure 3-3.

Figure 3-2: Flange making up the bottom of the liquid nitrogen reservoir. The substrate holding plate is bolted in with a glass sample tighyly secured. The thermocouple can be seen towards the top of the image mounted with a bolt.

3.2.1 Patterning the Resist with Resistive Heating

We selectively patterned the CO_2 mask by resistively heating a photolithographically predefined conductor on the substrate surface. OLEDs commonly feature a layer of the transparent conductor indium tin oxide (ITO), so we used that as a realistic testbed.

The power P through any circuit element is given by

$$P = IV \tag{3.1}$$

where I is the current passing through the element and V is the voltage across that element. By Ohm's law,

$$V = IR \tag{3.2}$$

where R is the resistance of the circuit element. The resistance depends on the

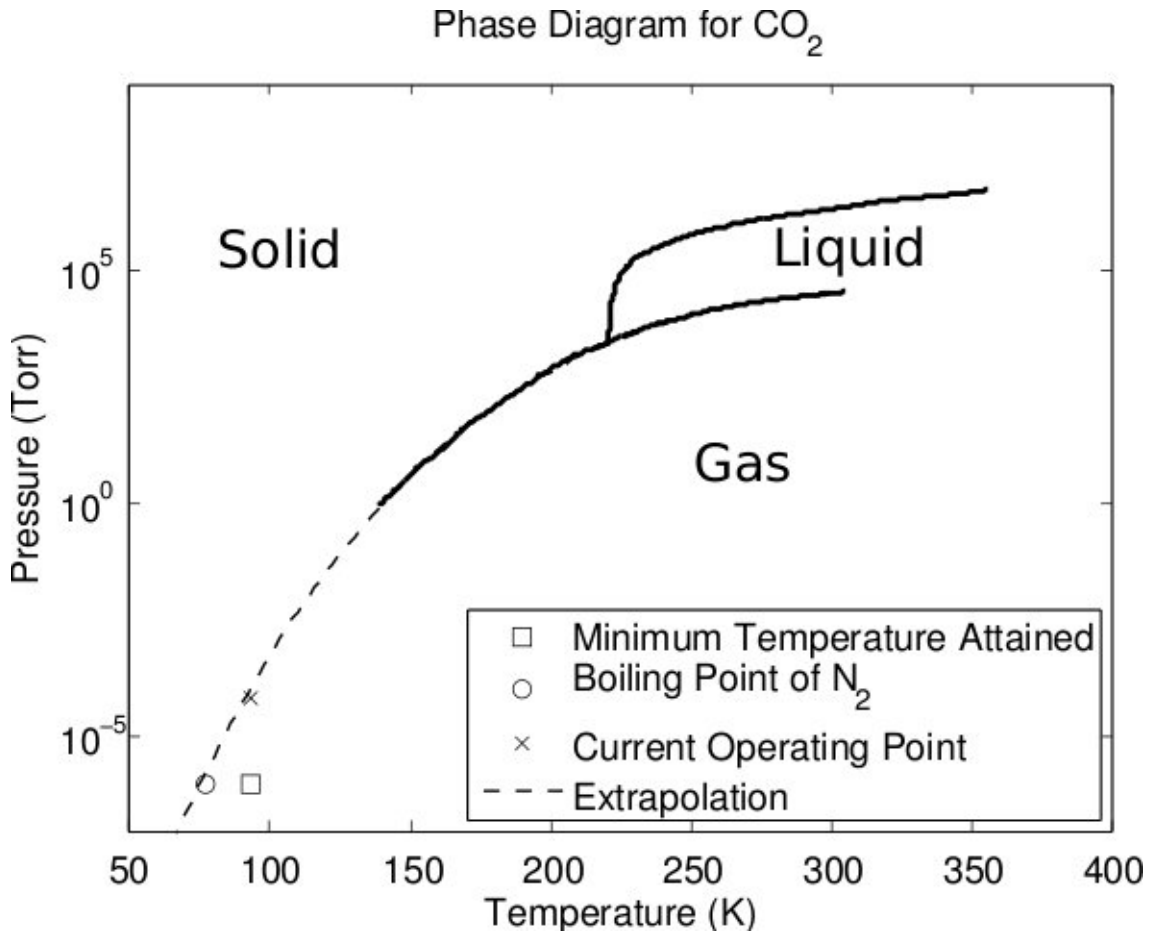

Figure 3-3: CO_2 phase diagram data[4], extrapolated by Nicholas Thompson for the low pressures and temperatures required for this process. Key points are noted.

resistivity ρ, the area A and the length l by the relation

$$R = \rho \frac{l}{A} \tag{3.3}$$

From equation 2.3, we find the amount of heat needed to sublime away a target region of CO_2 of mass m is

$$Q \approx mh_S = \int_0^{t_0} I(t)V(t)\mathrm{d}t = \int_0^{t_0} I^2(t)R\mathrm{d}t = \int_0^{t_0} I^2(t)\rho\frac{l}{A}\mathrm{d}t \tag{3.4}$$

As the ITO is essentially uniform in thickness D across the substrate and with pre-defined lines equal in width, this can be rewritten in terms of heat for a constant

thickness per unit width:

$$D\frac{Q}{w} \approx D\frac{mh_S}{w} = \rho l \int_0^{t_0} I^2(t)\mathrm{d}t \tag{3.5}$$

This leaves the current $I(t)$ as the only active process parameter, which can be run constant or pulsed accordingly to heat up and sublime away a desired mask region.

The ITO pattern used to test this selective sublimation method is displayed in figure 3-4. Three 100μm-wide lines allow for three 100μm-square subpixels. The six contact pads are wider, both to facilitate electrical contact and so current passed through a line will mostly heat the regions of highest resistance. The horizontal pad and center-right island allow for contact with a cathode laid across the top of all three subpixels. In this work, electrical contact in this work was made from the electrical feedthrough to the substrate's ITO pads in one of two ways: copper foil tape or small probe clips (shown in figure 3-5).

After a blanket deposition of CO_2 at 100Torr and $\sim$-165°C the chamber was pumped down to $\sim 10^{-5}$ Torr. At this temperature, the resistance of a single 100μm-wide line of the ITO used was about 500Ω. 100mA was pulsed through the line with a Keithley 2400 sourcemeter while the mask's selective sublimation was observed via the camera. 20nm of either tris(8-hydroxyquinolinato)aluminium (Alq_3), 4-(Dicyanomethylene)-2-tert-butyl-6-(1,1,7,7-tetramethyljulolidin-4-yl-vinyl)-4H-pyran (DCJTB) (see Appendix A) or silver was then thermally evaporated onto to the substrate (the choice of materials is explained below). We then vented the chamber to atmospheric pressure, and heated the sample with a thin $\sim$100W kapton heater (Omega Engineering) sandwiched between the substrate holder and liquid nitrogen reservoir. This forced the lift off of the CO_2 mask and the undesired regions of the thin film. This was observed by video to confirm complete sublimation. The pressure and temperature changes here reflect those in figure 2-2.

Alq_3 was chosen because it is a very well known OLED material (it was part of Tang and VanSlyke's first devices[39]). It is also has the advantage of obvious photoluminescence. DCJTB is another highly photoluminescent material that has

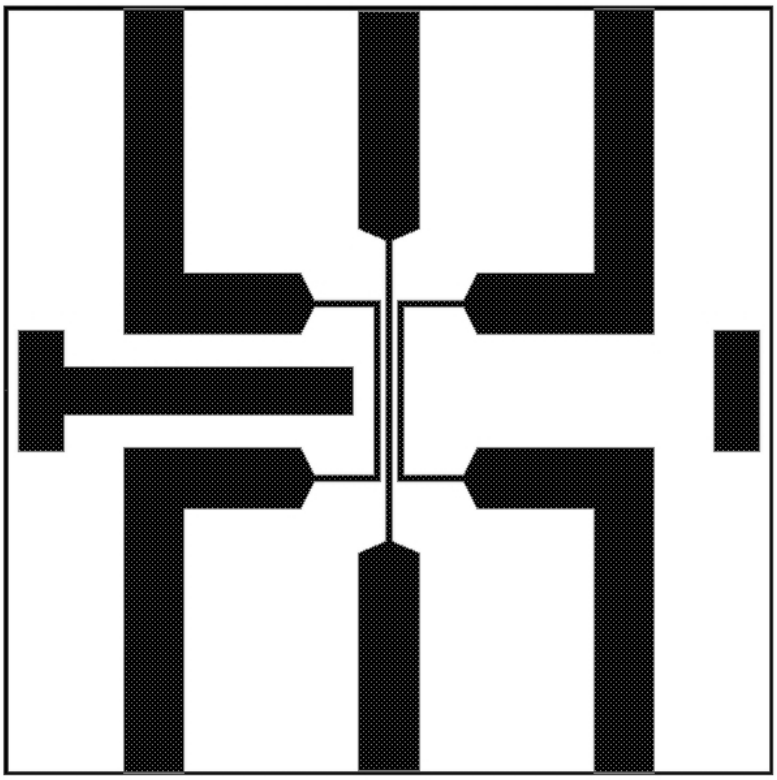

Figure 3-4: The pattern of the ITO used in resistive heating experiments. The black regions are ITO; the white regions are bare glass.

been used as a dopant with Alq_3 to produce red OLEDs[11]. An ultraviolet lamp highlights the pattern resulting from the experimental procedure above, as in figure 3-6. Because the copper foil tape used to make electrical contact floats, it is poorly cooled, so the adjacent regions show signs of CO_2 mask degradation. Figure 3-7 shows a micrograph of a similarly patterned line of silver. In both the images, the edges are fuzzy and the lines are not exactly 100μm wide. In large part this is because of the difficulties in fine calibration of power delivery by camera-mediated observation. A specially designed system would ameliorate the problem.

3.2.2 Patterning the Resist with a Stamp

We also investigated selective sublimation through direct stamping. A micron-featured stamp could heat specific regions of the mask through contact thereby patterning the mask. We chose the epoxy-based SU-8 photoresists to take advantage of their ver-

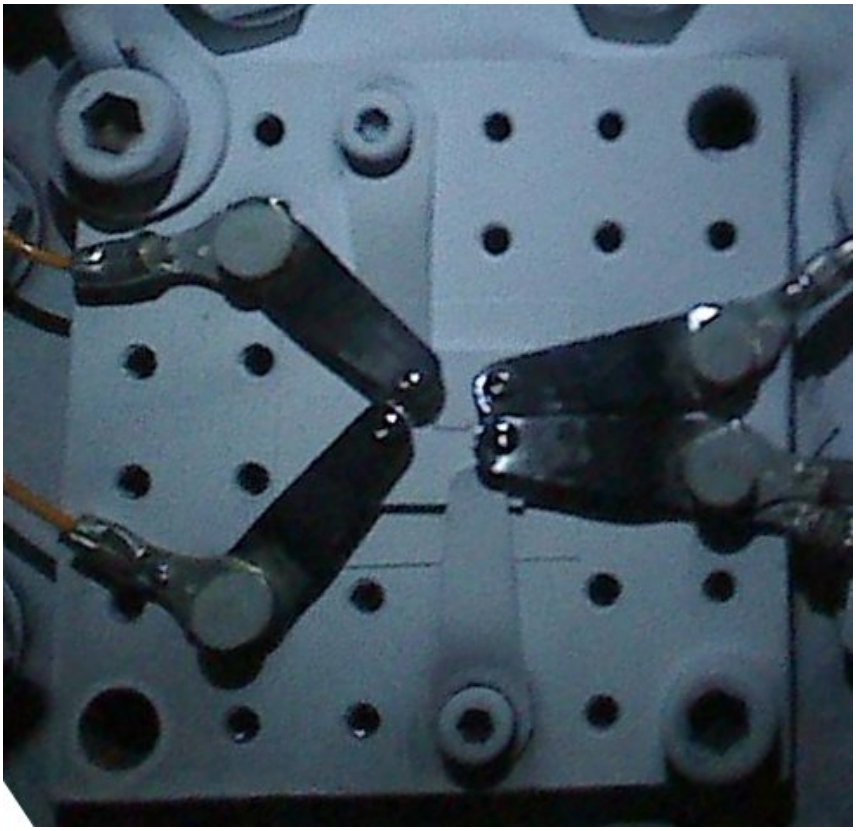

Figure 3-5: A mask of CO_2 patterned for a 100μm-wide line. The substrate holder is rigged with probe-tipped clips for electrical contact.

satility and rapid-prototyping capabilities: structures with thicknesses ranging from 1-600μm with aspect ratios as high as 20:1[2] that can be made in a matter of hours.

With stamping, the thermal energy required to sublime the CO_2 mask is, from equation 2.3,

$$Q = m(c_V \Delta T_{stamp} + h_S) \approx m h_S = m_{stamp} c_{V\,stamp} \Delta T_{stamp} \tag{3.6}$$

Here ΔT_{stamp} does not reflect the difference of initial temperatures between the mask and stamp, but rather the temperature change of the stamp after transferring energy to sublime away the mask. The heat transfer is a function of the stamping pressure and time, and if it is too great will sublime away necessary parts of the mask. To

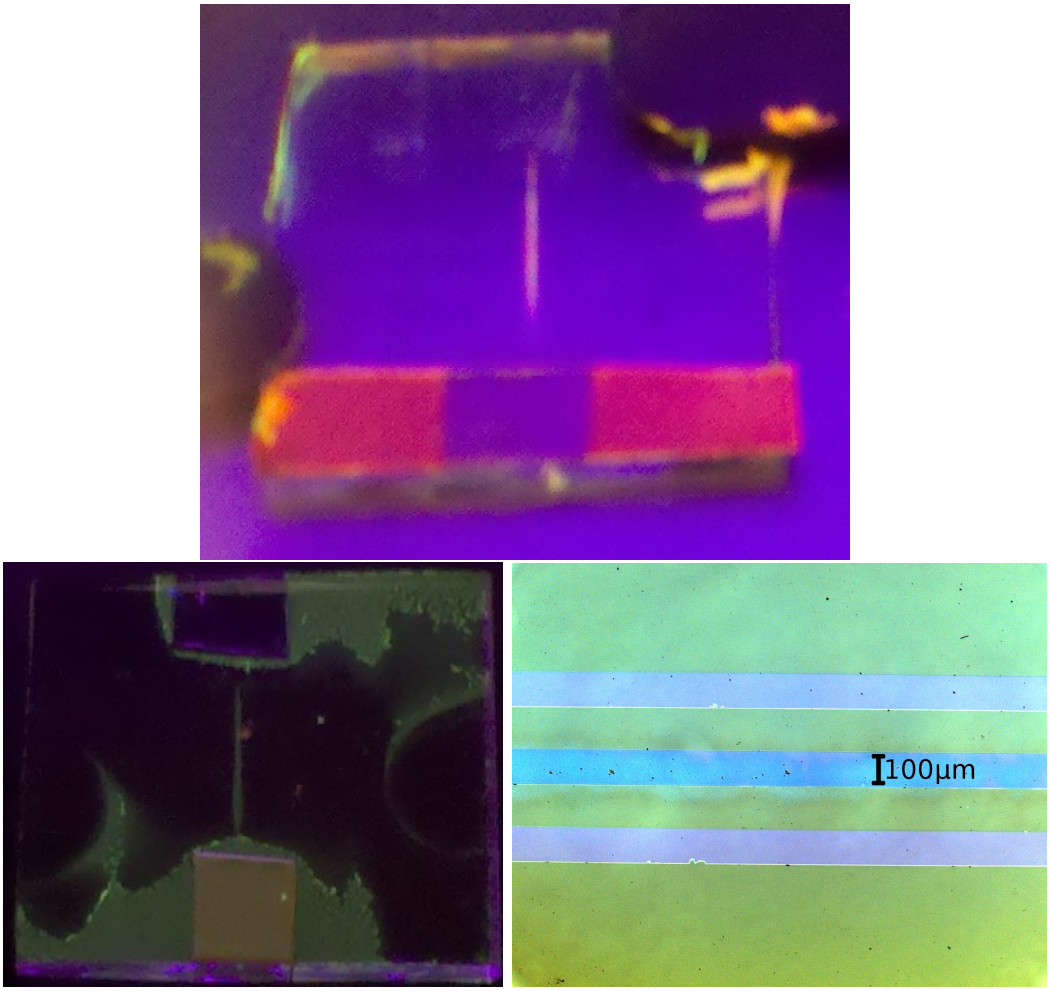

Figure 3-6: An exmaple of photoluminescence from a 100μm-wide line of DCJTB-doped Alq_3(*top*), and photoluminescence(*bottom-left*) and a micrograph(*bottom-right*) from a 100μm-wide line of Alq_3 patterned by resistive heating of ITO.

develop this further, we could use Fourier's law of conduction[30]

$$\mathbf{q} = -k\nabla T \tag{3.7}$$

with the relation for thermal diffusivity[30]

$$\alpha = \frac{k}{\rho c_V}, \tag{3.8}$$

where k is the thermal conductivity and ρ is the density. But until we can measure

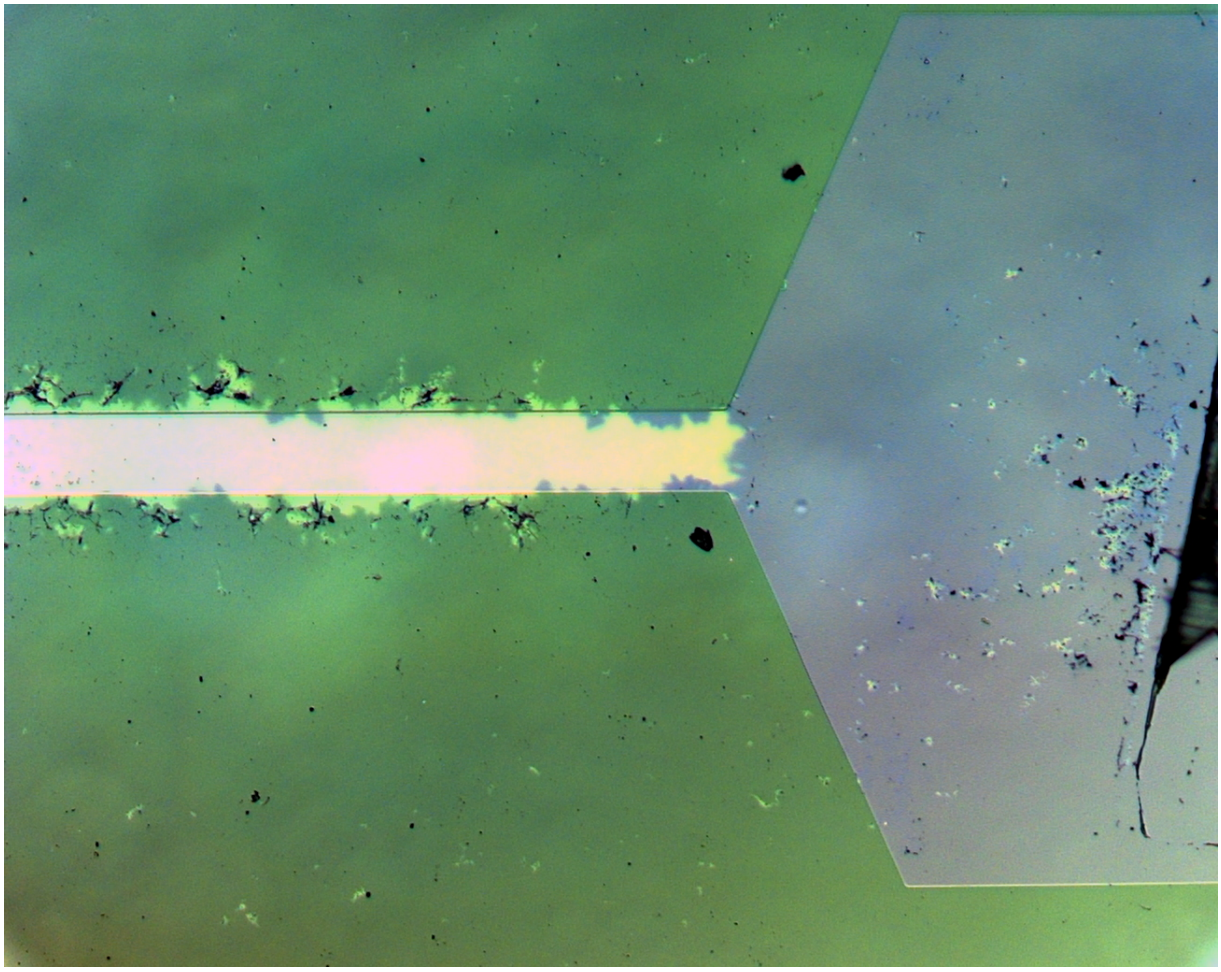

Figure 3-7: A micrograph from a 100μm-wide line of silver patterned by resistive heating of ITO

the thickness of the resist—and thereby estimate the surface area—this exercise is not illuminative.

We used SU-8 2150 obtained from Microchem to take advantage of its high thickness and aspect ratio potential—if the height of the features are not tall enough, we'd risk subliming away the entire mask. The resist was spun on solvent- and oxygen-plasma-cleaned silicon at 3000rpm to achieve features $\sim$115μm tall. A micrograph of these features can be seen in figure 3-8. After growing a blanket of CO_2 on the cold substrate, the stamp is pressed into the frozen CO_2 either by hand or by a linear solenoid mounted on a rotational feedthrough. After stamping, the thin film is deposited at pressures of $\sim 10^{-5}$ Torr. The mask is then lifted off, ideally taking the

undesired regions along with it. The last part still needs some optimization, as can be seen in figure 3-8.

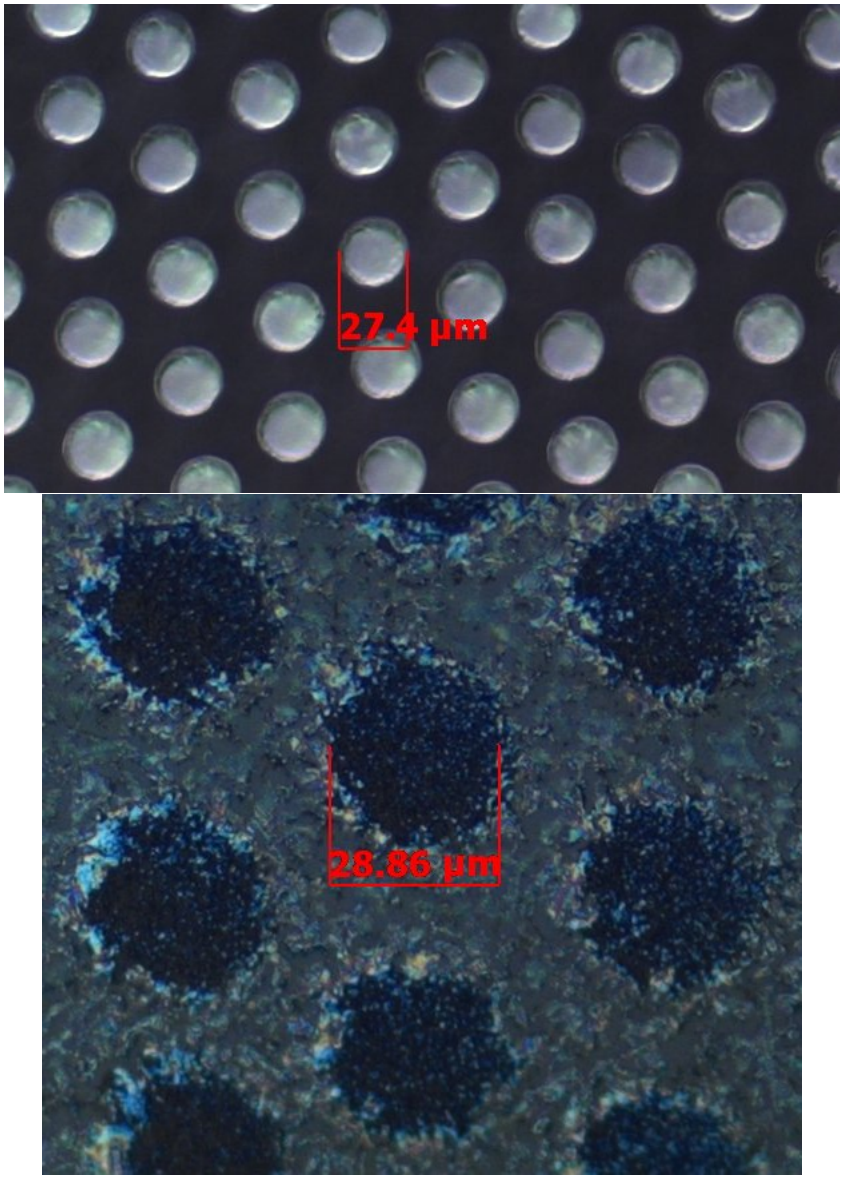

Figure 3-8: A micrograph of the 115μm-tall pillar SU-8 stamp(*top*) used to pattern circles of Alq_3(*bottom*)

Figure 3-8 suggests that either the heating fails to fully lift-off or—more likely—the stamping methods employed are inadequate. Our hands may slip, and our mechanical system is not yet so perfect as to prevent twisting and shifting that would thin or obfuscate the mask. The particular stamp's features may also have been too

short to make contact with the surface of the substrate without touching the rest of the mask.

3.3 Patterning the Resist Photolithographically

While patterning the resist photolithographically would seem to be the most elegant, for CO_2 this is impractical. A look at the absorption of solid CO_2 [23] shows strongest absorption at 2.7μm and 4.3μm. Overcoming both heat capacity and heat of sublimation of actively cooled CO_2 would require orders of magnitude more power than is currently available at those wavelengths—the time it would take to pattern a modern mother glass would be beyond unreasonable. For research and development at a small scale, it could be useful for rapid-prototyping purposes, but that has not yet been investigated.

Chapter 4

Conclusion

OLEDs must be capable of smaller features on a larger standard mother glass if they are to be cost-competitive with other display technologies. Current masking techniques have fallen short of meeting those goals, but sublimable masks are capable of filling the gap. We have used CO_2 to show that a sublimable mask can pattern thin films of both organic semiconductors and metals. We demonstrated two methods of mask definition: resistive heating of the underlying electrode and stamping. Both processes avoid the mask damage that plagues the FMM technique, but, unlike inkjet methods, don't constrain the deposition materials.

With the concept proved, the next step is to show that sublimable masks can deliver at a large scale. Commercial production requires accurate alignment to the substrate (each of the three subpixels is made of different materials), high device yield, and low takt time. The resistive heating method would require a restructuring of the driving backplane of the display, but 1-3μm alignment accuracy has already been shown for gravure cylinder and roll printing of electronics[29][34], and a cylinder etched deeply enough to stamp a CO_2 mask could work like the stamp in section 3.2.2. Cooling and heating could be pipelined to preserve takt time, but without test devices fabricated, yield cannot at this point be evaluated. Still, there is no reason to believe that substrate cooling during device growth would negatively affect OLEDs, which have been known to operate at cryogenic temperatures[17], and we foresee neither fundamental limitation to scaling this process up to larger substrates,

nor to achieving smaller feature sizes.

Appendix A

Molecules Used in this Work

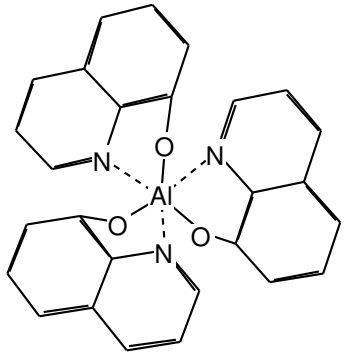

Figure A-1: Aluminium tris(quinolin-8-olate) (Alq_3)[6]

Figure A-2: Carbon dioxide (CO_2)

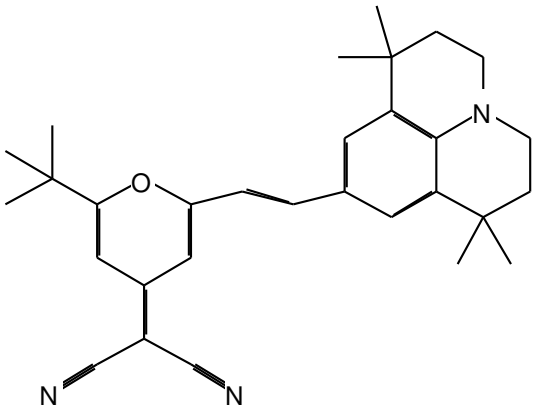

Figure A-3: 4-(Dicyanomethylene)-2-tert-butyl-6-(1,1,7,7-tetramethyljulolidin-4-yl-vinyl)-4H-pyran (DCJTB)[6]

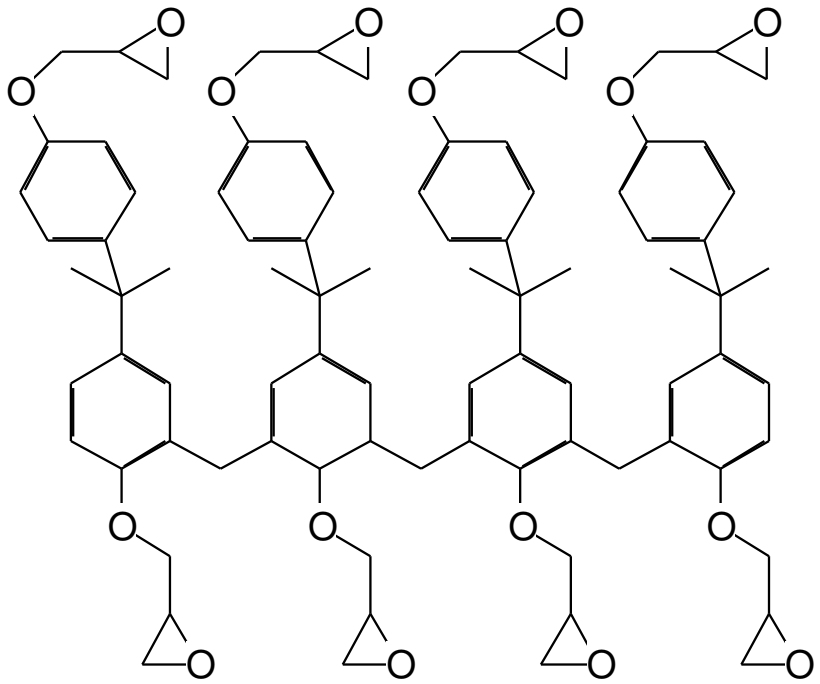

Figure A-4: SU-8 Photoresist[6]

Bibliography

[1] HTC mobile phone finder - browse by carrier, OS, and more. http://www.htc.com/us/products#/?1-2&sort=0.

[2] SU-8 resists, SU-8 2000, & SU-8 3000 resists - MicroChem. http://www.microchem.com/products/su_eight.htm.

[3] Apple - iPhone 4 - learn about the high-resolution retina display. http://www.apple.com/iphone/features/retina-display.html, 2010.

[4] CO2Tab: thermodynamic and transport properties of carbon dioxide. http://www.chemicalogic.com/co2tab/, 2010.

[5] Samsung smartphones | technology. http://www.samsung.com/au/smartphone/technology/super-amoled.html, 2010.

[6] xdrawchem chemistry editor, January 2011.

[7] D. Ambrose, R. M. Stephenson, and S. Malanowski. Handbook of the thermodynamics of organic compounds. 1987.

[8] M. A. Baldo, D. F. O'Brien, Y. You, A. Shoustikov, S. Sibley, M. E. Thompson, and S. R. Forrest. Highly efficient phosphorescent emission from organic electroluminescent devices. *Nature*, 395(6698):151–154, 1998.

[9] M. A. Baldo, M. E. Thompson, and S. R. Forrest. High-efficiency fluorescent organic light-emitting devices using a phosphorescent sensitizer. *Nature*, 403(6771):750–753, February 2000.

[10] Daniel Branton, Jene A. Golovchenko, Gavin M. King, Warren J. MoberlyChan, and Gregor M. Schrmann. Lift-off patterning processing employing energetically-stimulated local ..., April 2009. undefinedFiling Date: Dec 9, 2004 U.S. Classification: 216/41.

[11] C. H. Chen, C. W. Tang, J. Shi, and K. P. Klubek. Improved red dopants for organic electroluminescent devices. In *Die Makromolekulare Chemie. Macromolecular symposia*, page 4958, 1997.

[12] Jianglong Chen, Valrie Leblanc, Sung Hoon Kang, Paul J Benning, David Schut, Marc A Baldo, Martin A Schmidt, and Vladimir Bulovic. High definition digital fabrication of active organic devices by molecular jet printing. *Advanced Functional Materials*, 17(15):2722, August 2007.

[13] Roger Cheng. Samsung mobile display to boost 2011 production. *wsj.com*, September 2010.

[14] Jennifer Colegrove. DisplaySearch quarterly OLED shipment and forecast report. Technical report, DisplaySearch, 2010.

[15] Jennifer Colegrove and Calvin Hsieh. DisplaySearch OLED technology report. Technical report, DisplaySearch, 2011.

[16] JJ Cuomo, CR Guarnieri, KL Saenger, and DS Yee. Selective deposition with "Dry" vaporizable Lift-Off mask. *IBM Technical Disclosure Bulletin*, 35(1A), June 1992.

[17] Brian W. D'Andrade, James Esler, and Julie J. Brown. Organic light-emitting device operational stability at cryogenic temperatures. *Synthetic Metals*, 156(5-6):405–408, March 2006.

[18] Robert D. Deegan. Pattern formation in drying drops. *Physical Review E*, 61(1):475, January 2000.

[19] John A. DeFranco, Bradley S. Schmidt, Michal Lipson, and George G. Malliaras. Photolithographic patterning of organic electronic materials. *Organic Electronics*, 7(1):22–28, February 2006.

[20] D. R Gaskell. *Introduction to the Thermodynamics of Materials*. Hemisphere Pub, 2003.

[21] Bernard Geffroy, Philippe le Roy, and Christophe Prat. Organic light-emitting diode (OLED) technology: materials, devices and display technologies. *Polymer International*, 55(6):572–582, 2006.

[22] Anpan Han, Dimitar Vlassarev, Jenny Wang, Jene A. Golovchenko, and Daniel Branton. Ice lithography for nanodevices. *Nano Letters*, 10(12):5056–5059, December 2010.

[23] Gary B Hansen. The infrared absorption spectrum of carbon dioxide ice from 1.8 to 333 m. *Journal of Geophysical Research*, 102(E9):21,569–21,587, 1997.

[24] Hiroshi Hayase. DisplaySearch quarterly OLED shipment and forecast report. Technical report, DisplaySearch, 2010.

[25] Ha Soo Hwang, Alexander A. Zakhidov, Jin-Kyun Lee, Xavier Andr, John A. DeFranco, Hon Hang Fong, Andrew B. Holmes, George G. Malliaras, and Christopher K. Ober. Dry photolithographic patterning process for organic electronic

devices using supercritical carbon dioxide as a solvent. *Journal of Materials Chemistry*, 18(26):3087, 2008.

[26] WL Johnson, RB Laibowitz, and CC Tsuei. Condensed gas, in situ lithography. *IBM Technical Disclosure Bulletin*, 20(9), February 1978.

[27] Miyoung Kim. Samsung unit sees firm smartphone market. *Reuters*, May 2010.

[28] Gavin M. King, Gregor Schrmann, Daniel Branton, and Jene A. Golovchenko. Nanometer patterning with ice. *Nano Letters*, 5(6):1157–1160, June 2005.

[29] E. Kitazume, K. Takeshita, K. Murata, Y. Qian, Y. Abe, M. Yokoo, K. Oota, and T. Taguchi. 41.2: Development of polymer Light-Emitting diode (PLED) displays using the relief printing method. *SID Symposium Digest of Technical Papers*, 37(1):1467–1470, June 2006.

[30] S. Kou. *Transport phenomena and materials processing*. Wiley-Interscience, 1996.

[31] Jung-Ah Lee. In the lead–and trying to stay there. *wsj.com*, November 2010.

[32] Jung-Ah Lee. Samsung group to invest $38.3 billion in 2011. *wsj.com*, January 2011.

[33] D. R. Lide. CRC handbook of chemistry and physics. (Internet version 2011). *Boca Raton, FL: CRC*, 2011.

[34] Seung-Hee Nam, Soon-Sung Yoo, Youn-Gyoung Chang, Nam-Kook Kim, Yun-Hoo Kook, Jinook Kim, Chang-Dong Kim, Inbyeong Kang, and In-Jae Chung. 43.4: Enhancement of roll printing accuracy for TFT-LCD. *SID Symposium Digest of Technical Papers*, 39(1):648–650, May 2008.

[35] Tetsuro Ohtsuka, Masahide Tsukamoto, and Mitsuharu Tsuchiya. Liquid crystal matrix display. *Japanese Journal of Applied Physics*, 12(No. 3):371–378, 1973.

[36] Dora. Pesach and Abraham. Marmur. Marangoni effects in the spreading of liquid mixtures on a solid. *Langmuir*, 3(4):519–524, July 1987.

[37] James R. Sheats. Manufacturing and commercialization issues in organic electronics. *Journal of Materials Research*, 19(7):1974–1989, 2004.

[38] Max Shtein, Peter Peumans, Jay B. Benziger, and Stephen R. Forrest. Micropatterning of small molecular weight organic semiconductor thin films using organic vapor phase deposition. *Journal of Applied Physics*, 93(7):4005, 2003.

[39] C. W. Tang and S. A. VanSlyke. Organic electroluminescent diodes. *Applied Physics Letters*, 51(12):913–915, 1987.

[40] Kyoung Soo Yook, Soon Ok Jeon, Chul Woong Joo, and Jun Yeob Lee. Color stable and interlayer free hybrid white organic light-emitting diodes using an area divided pixel structure. *Synthetic Metals*, 159(17-18):1778–1781, September 2009.

[41] Alexander A. Zakhidov, Jin-Kyun Lee, Hon Hang Fong, John A. DeFranco, Margarita Chatzichristidi, Priscilla G. Taylor, Christopher K. Ober, and George G. Malliaras. Hydrofluoroethers as orthogonal solvents for the chemical processing of organic electronic materials. *Advanced Materials*, 20(18):3481–3484, 2008.